

Expression profile analysis to identify potential gene changes induced by dexamethasone in the trabecular meshwork

Miao Wei^{1,2}, Lu-Ming Chen¹, Ze-Yu Huang¹, Guo-Wei Zhang¹, Huai-Jin Guan¹, Min Ji¹

¹Eye Institute, Affiliated Hospital of Nantong University, Nantong 226001, Jiangsu Province, China

²Dalian Medical University, Dalian 116000, Liaoning Province, China

Correspondence to: Min Ji. Eye Institute, Affiliated Hospital of Nantong University, Nantong 226001, Jiangsu Province, China. amyji1234@hotmail.com

Received: 2022-01-26 Accepted: 2022-06-17

Abstract

• **AIM:** To investigate potential gene changes in trabecular meshwork (TM) induced by dexamethasone (DEX) in steroid-induced glaucoma (SIG).

• **METHODS:** The expression data of 24 cases from a public functional genomics data were sorted to identify the mechanisms of action of DEX on the TM. The relationships of the differentially expressed genes (DEGs) were enriched using Gene Ontology (GO) and Kyoto Encyclopedia of Genes and Genomes (KEGG) analysis. In addition, the hub genes were screened by the Search Tool for the Retrieval of Interacting Genes Database (STRING) and Cytoscape tools. Finally, human TM cells (HTMCs) were treated with DEX to preliminarily explore the function of hub genes.

• **RESULTS:** Totally 47 DEGs, including 21 downregulated and 26 upregulated genes were identified. The primary enriched results of the DEGs consisted of inflammatory response, extracellular matrix (ECM), negative regulation of cell proliferation, TNF signalling pathway and the regulation of tryptophan channels by inflammatory mediators. Subsequently, pro-melanin-enriched hormone (PMCH) and Bradykinin B1 receptor (BDKRB1) were screened as hub genes. It is verified in GSE37474 data set. Western blot and quantitative real-time polymerase chain reaction (qPCR) results showed that protein and RNA expression levels of BDKRB1 were significantly decreased after DEX treatment, while PMCH was not significantly changed.

• **CONCLUSION:** BDKRB1 may be a key gene involved in SIG onset, providing a suitable therapeutic target for improving the prognosis of SIG patients.

• **KEYWORDS:** dexamethasone; trabecular meshwork cells; steroid-induced glaucoma; differentially expressed genes; protein-protein interaction

DOI:10.18240/ijo.2022.08.03

Citation: Wei M, Chen LM, Huang ZY, Zhang GW, Guan HJ, Ji M. Expression profile analysis to identify potential gene changes induced by dexamethasone in the trabecular meshwork. *Int J Ophthalmol* 2022;15(8):1240-1248

INTRODUCTION

Steroid such as dexamethasone (DEX) are commonly used anti-inflammatory drugs to treat various ocular and systemic diseases^[1]. Although DEX has a vital role in treating many severe inflammatory diseases, its long-term use may increase the intraocular pressure (IOP) and lead to steroid-induced glaucoma (SIG)^[2]. When using ocular steroid hormones for treatment, approximately 30%-40% of people with normal blood pressure have increased IOP. Continuous IOP may cause damage to the optic nerve, resulting in loss of the visual field and ultimately blindness^[3]. Increased IOP is a recognized risk factor for glaucoma, but the mechanisms underlying steroid-induced ocular hypertension are currently unclear. Researchers have shown that its pathogenesis is similar to that of primary open angle glaucoma (POAG)^[4].

Researchers have found that SIG is mainly caused by the accumulation of fibronectin (FN) and type IV collagen outside the trabecular meshwork (TM)^[5]. In all steroid glaucoma specimens, basement membrane-like substances can be seen near the trabecular lamellae at the ultrastructural level, and unrecognized thin fibre deposition bands can be seen in the subendothelial area of Schlemm's canal (SC)^[6]. DEX changes the structure of TM by increasing trabecular cell rigidity. Under the influence of DEX, the matrix deposited by TM cells is approximately four times more organized, and it is more rigid than the matrix in healthy eyes. Extracellular matrix (ECM) proteins are expressed at high levels, such as fibrillin and myocilin (MYOC)^[3]. Biochemical and genetic studies have shown that the main feature of the TM-induced glucocorticoid

Table 1 Characteristics of the included microarray datasets

GSE ID	Participants	Tissues	Analysis type	Platform	Year
GSE124114	9 cases and 9 controls	TM	Array	GPL6244	2018
GSE65240	3 cases and 3 controls	TM	Array	GPL14550, GPL17077	2015
GSE37474	5 cases and 5 controls	TM and corneoscleral tissue	Array	GPL570	2012

TM: Trabecular meshwork.

response (TIGR) is the altered expression of trabecular muscle protein, which plays a vital role in the mechanism of SIG^[4]. Moreover, the molecular changes of TM may increase the resistance to the outflow of aqueous humour, which may be an important reason for the occurrence of SIG. However, its pathogenesis is not fully understood. Therefore, understanding the pathological changes in the TM microstructure induced by DEX treatment is essential for the development of effective therapies^[7].

To date, many studies have employed a variety of experimental methods [such as RNA sequencing (RNA-seq)] to select differentially expressed genes (DEG) profiles of TM after exposure to steroid hormones at the whole genome level, resulting in complex and comprehensive datasets^[8]. Systematically and comprehensively analysing the relationship between DEGs and differentially activated signalling pathways in DEX-treated and nontreated samples will help us gain new insights into the progression and treatment of SIG. Therefore, the existing gene expression datasets can be used as a powerful tool to identify the biomarkers of genetic changes in the TM caused by DEX and help guide their diagnosis or better plan the treatment of SIG patients.

It is generally believed that increased IOP caused by changes in the structure of TM can cause visual impairment, and the gradual increase in IOP makes it challenging to diagnose SIG^[3]. Therefore, it is the first task to study the pathogenesis of glaucoma caused by DEX and to develop better diagnosis, treatment and prevention strategies. To achieve this, two Gene Expression Omnibus (GEO) datasets (GSE124114 and GSE65240) were analysed to obtain DEGs. R language software was used to extract, analyze and sequence the gene expression matrix^[9]. In order to study the biological classification of the 47 DEGs, gene enrichment analysis was performed using the DAVID website. Moreover, we explored a protein interaction network (PPI) containing these genes and analyzed the network using the molecular complexity detection (MCODE) program to identify essential gene modules. We used GSE37474 to verify the hub genes PMCH and BDKRB1. We treated human TM cells (HTMCs) lines exposed to DEX for one, three and seven days and then detected the expression levels of the seed genes^[10]. These results were visualized and compared to reveal specific molecular processes induced by corticosteroids. These processes can be used to further explore targeted drug therapy and SIG mechanisms.

MATERIALS AND METHODS

Microarray Data and Data Collection As shown in Table 1, three datasets (GSE124114^[11], GSE65240^[10], and GSE37474) were downloaded from a public functional genomics data repository, known as GEO. We use R language software (R Foundation for Statistical Computing, Vienna, Austria) to transform the probes of these three datasets into corresponding genetic symbols.

GSE124114 and GSE37474 utilize the GPL570 platform, which has the complete human genome with U133 sets and 6500 additional genes for analysis of more than 47 000 transcripts. GSE65240 utilizes the GPL14550 platform, including the Agilent Probe Names and GPL17077 (Agilent-039494 SurePrint G3 Human GE). The GSE124114 dataset includes nine experimental samples and nine control samples, and all paired samples were collected from the same donor. GSE65240 includes three experimental samples and three control samples. GSE37474 contains five DEX treatment samples and five non-DEX treatment samples. All samples were obtained from 5 paired donor eyes.

Identification of Differentially Expressed Genes Gene expression sequencing data and patient clinical information were obtained from the GEO database (<https://dcc.icgc.org/>) for the corresponding specimen. R software was then used to extract and sequence the information^[12]. Significant analysis of microarray (SAM) was used to screen the significantly changed genes with false discovery rate (FDR) <0.05 and log₂ FC ≥1. Heatmaps and volcano plots were drawn in R. DEGs were up- and downregulated if log₂ FC values were >0 and <0, respectively. The intersection of different genes in the two datasets was used to draw a Venn diagram.

Functional Annotation of Differentially Expressed Genes Gene Ontology (GO) and Kyoto Encyclopedia of Genes and Genomes (KEGG) enrichment analyses were used to annotate the structure, functions, and pathways of the DEGs. To obtain further insights into the comprehensive function of the DEGs, DAVID was performed^[13]. KEGG and GO are significant bioinformatics tools used to link genomic information with higher-order functional information^[14-15]. Finally, the enrichment of GO terms and KEGG signalling pathways was presented and based on the criteria of FDR <0.05.

Protein Interaction Network Construction Import 47 DEGs into the STRING database (version 11.0; <https://stringdb>).

org/), a web tool for exploring protein interactions, with the advanced option set to ≥ 0.4 ^[16]. Analysing the functional interactions between the proteins may provide insights into the mechanism of disease occurrence and development. This network was reconstructed *via* Cytoscape software (version 3.8.2), a free visualization software. Cytoscape's plug-in Molecular Complexity Detection (MCODE, version 2.0.0) was used to explore the significant modules in the PPI network that cluster a given network based on the topology and find tightly related areas^[17].

Hub Genes Selection and Validation Among the 47 genes, five genes of interest (*PMCH*, *BDKRB1*, *HTR2B*, *GRP*, and *PIK3R1*) have not previously been studied in the context of DEX-induced genetic changes in TM cells and were thus verified in another dataset, GSE37474, downloaded from the GEO database. In the GSE37474 dataset, from the eyeballs of 5 donors, one eye in each pair was infused with a medium containing 100 nmol/L DEX, and the other eye was only in the medium as a control. Under the same conditions, both eyes remained open for 10d. After 10d in culture, the TM and the underlying corneoscleral tissue were dissected along Schwalbe's line and the scleral spur. The RNA was extracted using Uneasy minipreps (Qiagen).

Cell Identification and Treatment Primary HTMCs (sciencell, 6590) were cultured in TM cell medium (sciencell, 6591) with 10% foetal bovine serum (FBS) and 1% penicillin-streptomycin (PS; Gibco, Thermo Fisher Scientific, Waltham, USA). All HTMCs were deposited in a constant atmosphere with 5% CO₂ and 95% air at 37°C. All experiments use HTMCs of generations 4-8. The HTMCs was planted in 24-well plates (with slivers placed in the plates) with culture medium and then placed in an incubator for culture. Cell identification was carried out after the growth and fusion reached 80%. Cell immunofluorescence technique (ICC) was used to stain the mesenchyma cells on the sliver of 24 well plate. To verify the effect of DEX on the HTMCs, they were cultured in 6-well plates^[18]. One group was not processed, and the remaining two groups were cultured for one, three and seven days in dimethyl sulfoxide (DMSO, 0.1%) and DEX (100 nmol/L) dissolved in 0.1% DMSO^[19].

Immunofluorescence Spread the 4th generation HTMCs in a 24-well plate and discard the medium when it is full. PBS solution cleaning 3 times, 4% polyformaldehyde room temperature fixed 30min, PBS solution cleaning 3 times, 5min each time, add closed liquid, room temperature closed 2h. Finally, an anti-rabbit polyclonal COL-IV antibody (1:200, proteintech, Shanghai) was added overnight at 4°C. Day 2 recycle one resistance, add the PBS solution to clean 3 times, add two resistance to it, and incubate 2h at room temperature. After washing the cells with a PBS solution, seal the tablet

with a reagent containing 4',6-diamino-2-benzene pyridium (DAPI). Fluorescence is detected with a confocal microscope (Leica, Germany) or a fluorescence microscope (Leica).

RNA Extraction and Quantitative Real-time Polymerase Chain Reaction In order to further confirm the findings from the bioinformatics analysis, primary HTMCs were cultured for reverse transcription-polymerase chain reaction verification. TRIzol reagent (Invitrogen, Carlsbad, CA, USA) was applied to extract total RNA from the HTMCs. The RNA sample was reverse transcribed into cDNA with specific primers (Funglyn Biotech, Shanghai, China; *BDKRB1*: forward primer: ATCAACGGGGTCATCAAGGC, reverse primer: ATGGATCGCAGCAGGAATGT), and the data were normalized to GAPDH (forward sequence GTCTCCTCTGACTTCAACAGCG, reverse sequence ACCACCCTGTTGCTGTAGCCAA). The expression of GAPDH was measured as an internal control. We determined relative gene expression by the comparative 2^{- $\Delta\Delta C_T$} method, and $P < 0.05$ indicated statistical significance.

Western Blot HTMCs are lysed for 30min in a 4°C lysis buffer (RIPA lysate: protease inhibitor s100:1; Solarbio, Beijing, China). Protein concentrations are measured using the BCA kit (Pierce, Thermo Fisher). In addition, protein samples are separated by a sodium alkyl sulphate-polyacrylamide gel electrophoresis (SDS-PAGE) gel (16 μ g each) and transferred to a PVDF membrane (Thermofis Technologies). Block the cell membrane for 2h with 5% skimmed milk in tris buffer salt water containing Tween 20. This was followed by anti-BDKRB1 (A1959, 1:1000, Abclonal, Shanghai), anti-myocilin (14238-1-AP, 1:1000, proteintech, Shanghai) and anti-GAPDH (3777R-30T, 1:2000; Bio Vision, Inc., Shanghai, China) fought overnight at 4°C. Normalize protein expression levels with GAPDH. The membrane was then incubated at room temperature of 2h with the horseradish peroxidase (HRP) labeled goat anti-rabbit II (1:10 000). Repeat the experiment 3 times, using Image J software analysis.

Statistics All statistical calculations were performed using SPSS 11 statistical software. The statistical significance of differences between the two groups was analyzed using a *t*-test based on the data distribution characteristics. A P value < 0.05 was considered statistically significant.

RESULTS

Identification of DEGs Between the Experimental and Normal Controls Raw data from two independent datasets (GSE124114 and GSE65240) were obtained from GEO; DEGs (236 in GSE124114 and 882 in GSE65240) were identified using R language. The differential gene expression between DEX-treated samples and control samples was displayed by heatmap visualization (Figure 1A, 1B). These DEGs were visualized in volcano plots (Figure 1C, 1D). In addition, the

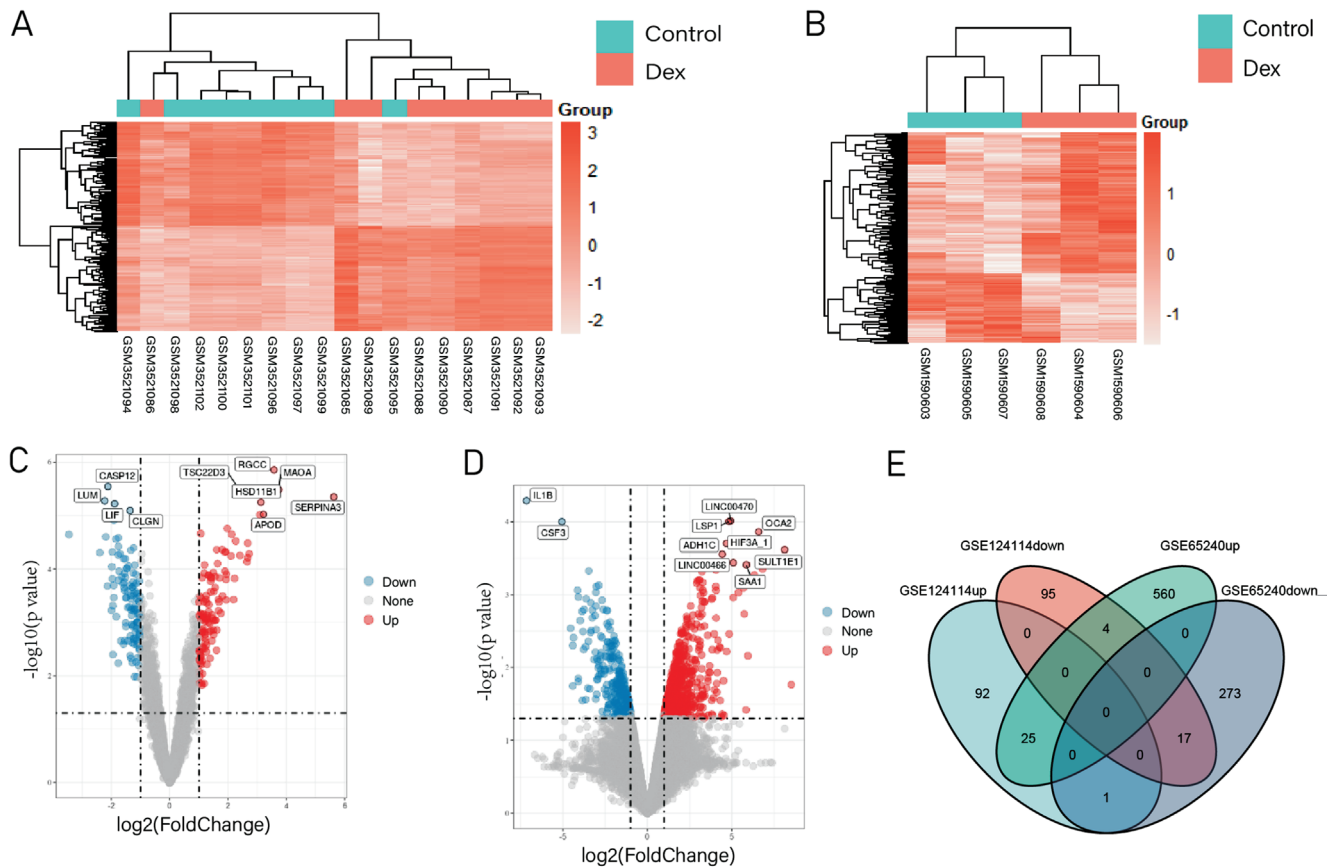


Figure 1 Differential expression of genes in the two sets of samples A, B: Heatmap of the DEGs screened by the limma package. The horizontal axis shows samples of microarray data, and the vertical axis shows DEGs. C, D: Volcano plots of DEGs. Red points represent up-regulated genes screened on the basis of fold change >1.0 and a corrected $P < 0.05$. Blue points represent down-regulation of gene expression screened on the basis of fold change <1.0 and a corrected $P < 0.05$. Gray points represent genes with no significant difference. E: DEGs were selected with a $|\text{fold change}| > 1$ and $P < 0.05$ among the mRNA expression profiling sets GSE124114 and GSE65240. The two datasets exhibited an overlap of 47 genes. DEGs: Differentially expressed genes.

intersecting function indicated that 47 DEGs were commonly dysregulated (21 down- and 26 upregulated DEGs from two independent datasets) using the Venn diagram package in R ($\log \text{FC} > 1$; Figure 1E).

Gene Ontology Enrichment and KEGG Pathway Analysis of DEGs Through DAVID analysis, the results of the GO analysis showed that the variation of DEGs related to biological processes significantly focuses on the negative regulation of angiogenesis, inflammation and cell proliferation. DEGs related to cell composition are mainly concentrated in the composition of extracellular space, extracellular region and plasma membrane. In terms of molecular functions, the DEGs were significantly enriched in cytokine activity, transport activity, receptor binding and growth factor activity, as shown in Figure 2A. The analysis of the KEGG pathway shows that the typical top pathways related to the DEGs are the regulation of the tryptophan pathway by inflammatory mediators, the tumour necrosis factor signalling pathway, the VEGF signalling pathway, the HIF-1 signalling pathway and the Jak-STAT signalling pathway, as shown in Figure 2B.

Modular Analysis via the DEGs Protein-protein Interaction Network Through the STRING website, we constructed and visualized a PPI network of the DEGs (Figure 2D). A total of 47 nodes and 25 edges were identified in the PPI network. The most powerful module was obtained using Cytoscape, as shown in Figure 2D. GO/KEGG enrichment analysis was performed using the DAVID website, identifying the hub genes as *PMCH*, *BDKRBI*, *GRP*, *HTR2B* and *PIK3R1*. These results show that these genes are mainly enriched in cell division and mitosis, nuclear division and the cell cycle (Table 2).

Validation and Efficacy Evaluation of the Hub Genes In the GSE124114 and GSE65240 datasets, five genes of interest, *PMCH*, *BDKRBI*, *GRP*, *HTR2B* and *PIK3R1*, were identified (Figure 3A, 3B). Their expression in the DEX treatment group was significantly altered relative to the controls. The expression levels of the above five candidate genes were studied in another dataset, GSE37474 (Figure 3C). In the GSE37474 dataset, compared with the control group, the expression of *PMCH* and *BDKRBI* in the DEXe group was significantly downregulated (all $P < 0.01$), but there was no

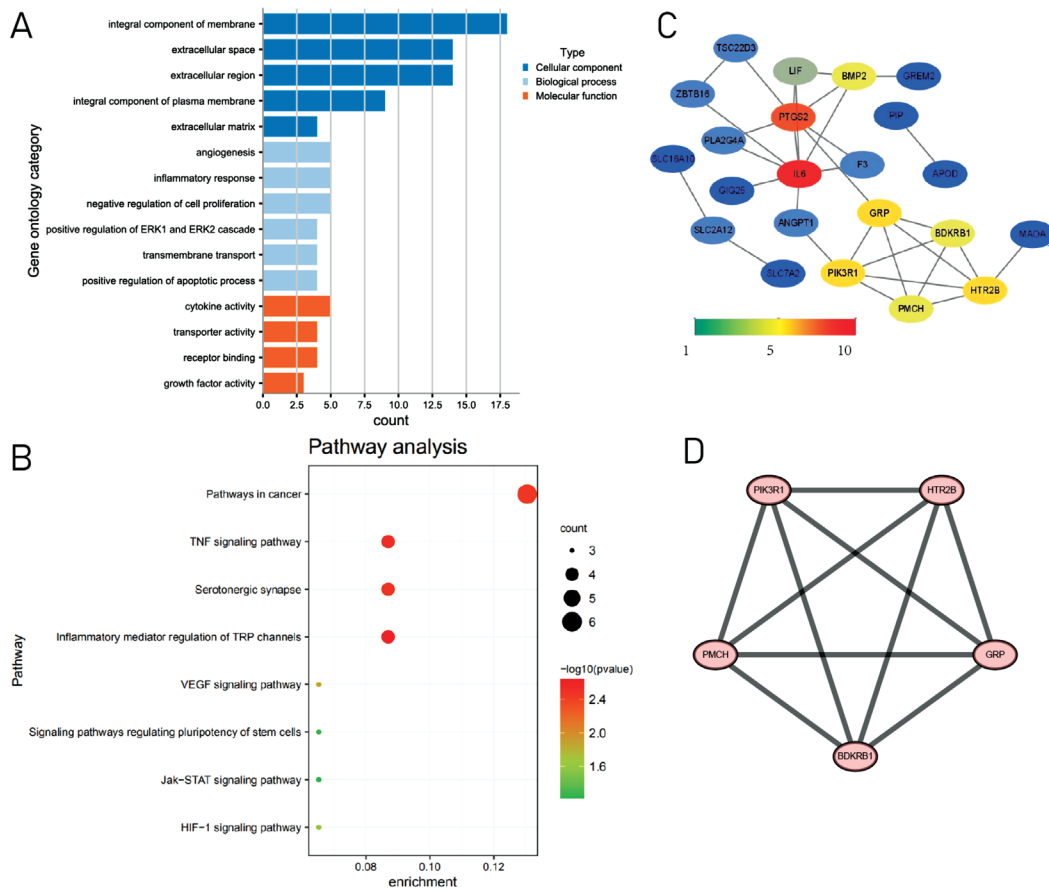


Figure 2 Interaction network and analysis of differential expression of genes A: Gene ontology (GO) enrichment analysis of DEGs, namely biological processes, cellular components and molecular functions; B: Enriched pathways of DEGs, the color indicates the significant degree of enrichment and the size indicates the number of genes enriched for each result; C: Protein-protein interaction network (PPI) of DEGs. The color indicates the number of proteins interacting with the other proteins; D: The top 1 module in MCODE.

Table 2 The GO enrichment analysis and KEGG pathway enrichment analysis of the Top 1 module

GO	Description	P
GO:0014065	Phosphatidylinositol 3-kinase signaling	0.006417
GO:0007205	Protein kinase C-activating G-protein coupled receptor signaling pathway	0.007365
GO:0007218	Neuropeptide signaling pathway	0.023845
GO:0007268	Chemical synaptic transmission	0.045961
hsa04750	Inflammatory mediator regulation of TRP channels	2.01E-04
hsa04020	Calcium signaling pathway	0.031369
hsa04810	Regulation of actin cytoskeleton	0.040128
hsa04080	Neuroactive ligand-receptor interaction	0.048919

significant difference in the expression of *GRP*, *HTR2B* and *PIK3R1*. Therefore, we speculate that *PMCH* and *BDKRB1* are potential biomarkers of SIG.

Expression of HTMCs Morphology and Biomarkers

Under the microscope: cell morphology is elliptical, shuttle-shaped, *etc.*, similar to fibroblasts, cell nucleus is oval or circular, contains a large amount of cytoplasm, and contains a small amount of pigment particles (Figure 4A). Cell growth is slow, generally 3 to 5d cells fusion, after transmission of cell growth speed and cell density. HTMCs currently lacks specific markers, and we chose the small beam mesh biomarker

collagen IV (col IV) protein for small beam mesh cell identification. Immunofluorescence results showed that small beam mesh cells expressed col IV protein.

Hub Genes BDKRB1 RNA were Low in the Experimental Group

The biological analysis results suggest that *BDKRB1* and *PMCH* play a vital role in the development of TM structural changes. To verify the association between hub genes and SIG, we confirmed the expression of *BDKRB1* and *PMCH* by PCR. Compared with the experimental and DMSO groups, there was low expression of the *BDKRB1* gene in HTMCs after DEX treatment (Figure 4C) and no significant

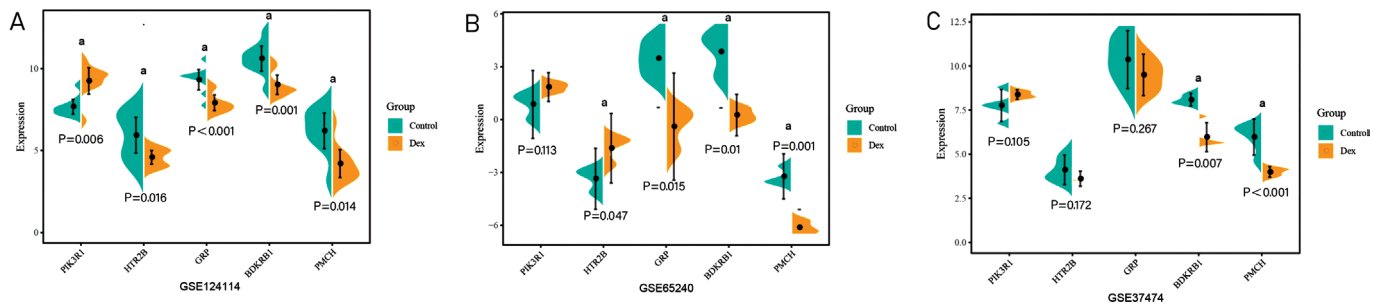


Figure 3 Expression of hub genes in datasets A, B: The expression of 5 hub genes in DEX treatment TM tissues and non-DEX treatment TM tissues. Compared to the normal samples, *PIK3R1* and *HTR2B* expression was increased, and *GRP*, *BDKRB1* and *PMCH* were decreased in DEX-treatment samples. C: The expression of 5 hub genes in GSE 37474. Compared to the non-DEX treatment TM tissues, *PIK3R1*, *HTR2B* and *GRP* were no significant change, *BDKRB1* and *PMCH* were decreased in DEX -treatment samples. ^a $P < 0.05$ compared with the control group.

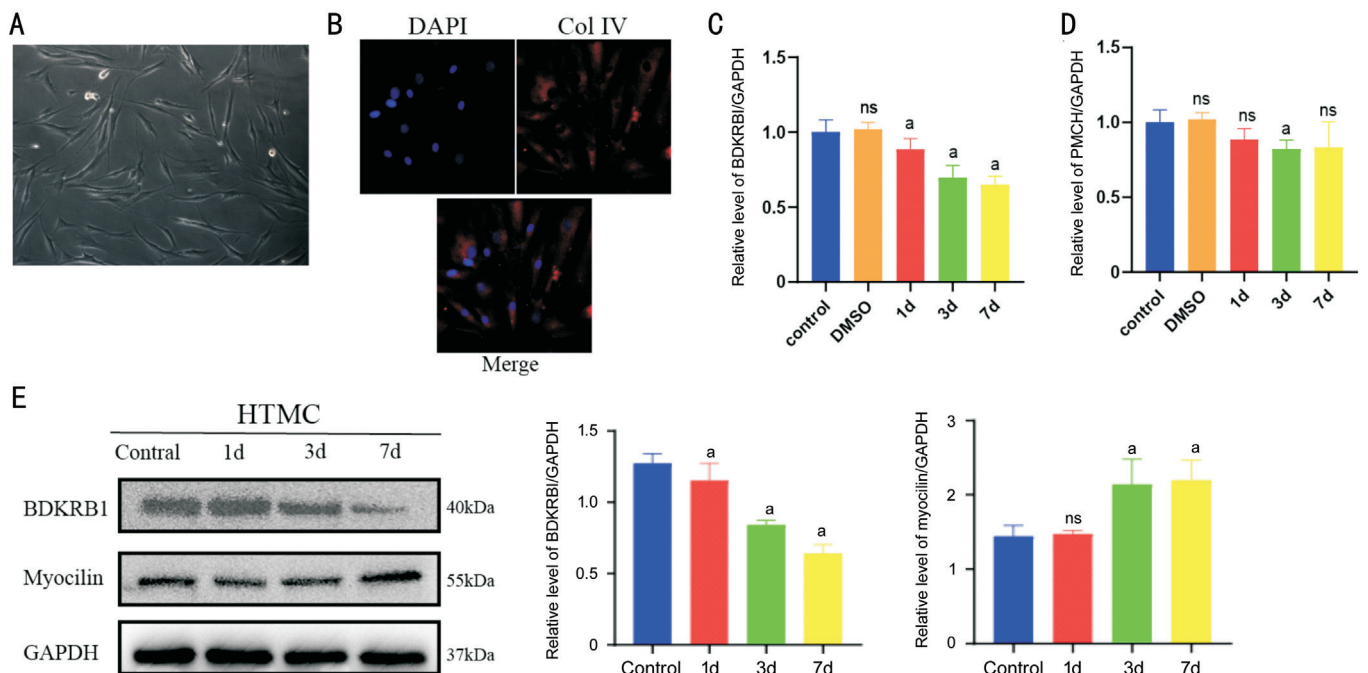


Figure 4 The expression of hub genes in HTMCs A: The microscope looks at the HTMCs pattern; B: HTMCs biomarkers: DAPI (blue), collagen 4 (red), bar=50 $\mu\text{mol/L}$; C: *BDKRB1* were down-regulated in DEX treatment HTMCs; D: There was no significant difference in *PMCH*; E: The bands of myocilin and *BDKRB1* proteins and quantification analyses of myocilin and *BDKRB1* expression levels. ^a $P < 0.05$ compared with the control group.

difference in *PMCH* (Figure 4D). According to western blot experiment, the expression level of *BDKRB1* was significantly reduced in the experimental group. These results indicate that the *BDKRB1* plays an important role in DEX-induced SIG compared with the standard group.

Dexamethasone Induces the Expression of Myocilin and *BDKRB1* Proteins in HTMCs Dexamethisone can induce the expression of myocilin protein in small beam mesh cells, so we compared the expression of myocilin protein in dexamethisone induced HTMCs to further identify whether the above cells are small beam mesh cells. Western blot shows a significant increase in the expression of Myocilin protein in HTMCs after 7d of treatment (Figure 4E). In addition, after 3d of dexamethisone-induced small beam mesh cells, *BDKRB1*

expression decreased and significantly decreased by day 7 (Figure 4E). The strength of the stripe was quantitatively analyzed using Image J to find that dexamethisone induced the expression of Myocilin and *BDKRB1* proteins ($P < 0.05$; Figure 4E).

DISCUSSION

How DEX causes glaucoma has been difficult to explain. Early studies showed that steroids have an essential relationship with POAG. Various researchers have shown that patients with POAG are more likely to develop steroid-induced OHT, and patients with corticosteroid reactions are at a higher risk of POAG^[20]. It has been reported that cortisol levels in the plasma and AH of POAG patients are elevated, and changes in cortisol metabolism were found in TM cells obtained from POAG

patients^[21-22]. Everyone has a different degree of response to steroid treatment: compared with 40% of the general population, 90% of glaucoma patients respond to steroids^[23]. The increase in IOP usually occurs several weeks to several months after initiation of the steroids, and the degree of growth depends on the potency and dose of the steroids^[19,24]. Even if the steroid treatment is stopped, the IOP may continue to rise, and sometimes the glaucoma requires surgery to control the IOP^[2]. This study analyzed the DEGs in the GSE124114 and GSE65240 datasets and identified 47 DEGs after the intersection, including 21 downregulated genes and 26 upregulated genes. Then, the 47 integrated DEGs were subjected to biological process (BP), cellular component (CC) and molecular function (MF) analyses. The DEGs were significantly enriched in angiogenesis, inflammatory response, negative regulation of cell proliferation (GO: BP), ECM (GO: CC), cytokine activity, and transport activity (GO: MF). Steroids affect the cell cycle, but this effect differs by the dose of steroids and the cell type. Guichard *et al*^[25] observed the effects of different corticosteroids on the hyperproliferation of keratinocytes and found that all corticosteroids reduced cell proliferation. However, the proliferation of cultured corneal epithelial cells increases when the DEX concentration of betamethasone is less than 10^{-6} M, while cell proliferation is inhibited when the concentration of DEX is greater than 10^{-4} M^[26]. Moreover, the Bogarin *et al*^[27] used primary scleral fibroblasts to study the steroid response of TM distal cells and found that compared with the control group, DEX-treated cells proliferated slower, migrated less, and showed more senescence. Some clinical studies have found that elderly subjects have a higher risk of increased IOP after using DEX eye drops, and their odds ratio for glaucoma is 1.72^[28].

In addition to the cell cycle, ECM studies are also very extensive. The ECM is the most abundant component in the TM. The ECM of the TM seems to be a source of potential growth factors and other small regulatory molecules, and its activity needs to be strictly regulated^[29]. Previous studies have shown that in an organ culture model supplemented with DEX, the ECM deposition by TM increases, and many ECM components in the TM change to varying degrees, such as MMP2, MYOC, and FN^[30-31]. Growth differentiation factor-15 (GDF-15) is a common component of the ECM derived from HTMCs and it has been confirmed to be distributed in the outflow tract of normal human aqueous humour. DEX can significantly increase the GDF-15 protein level in human TM cells. Stimulating HTMCs with GDF-15 can significantly increase the formation of actin stress fibres and focal adhesions, myosin light chain phosphorylation, gene expression and the levels of ECM proteins and α -smooth muscle actin (α -SMA)^[32]. In short, the ECM and cell cycle may play a

role in the homeostasis of normal eyes and imbalances lead to glaucoma and IOP.

KEGG pathway analysis demonstrated that these integrated DEGs were enriched in the following three pathways: inflammatory mediator regulation of transient receptor potential (TRP) channels, TNF signalling pathway, and VEGF signalling pathway. Studies have shown that TRP channels are potential sensors and transducers of inflammatory pain and they participate in matrix homeostasis through the regulation of metalloproteinases and 1A1 collagen^[33]. It is boldly speculated that the TRP pathway may be involved in the remodelling of the ECM of the TM to mediate the occurrence of SIG. When laser trabeculoplasty is used to treat POAG, the cytokine TNF increases the protein levels of matrix MMP-3 and MMP-9, and the increase in MMP-3 plays a crucial role in the success of the treatment^[34]. Therefore, we need further experiments to verify the roles of these pathways, which will help elucidate the mechanism of SIG.

The occurrence and development of SIG are inseparable from the participation of inflammation^[35]. Fini *et al*^[35] identified the expression of the inflammatory marker endothelial leukocyte adhesion molecule-1 (ELAM-1) as the defining feature of the open-angle and angle-closure TM phenotypes of hypertensive glaucoma. This further proves that the expression of ELAM-1 is activated by the IL1A/nuclear factor- κ B (NF- κ B) inflammatory pathway, which is of great significance in the TM tissue of high IOP glaucoma.

The kallikrein-kinin system (KKS) is an endogenous metabolic cascade that dominates a broad spectrum of physiological events, including inflammation, ischaemia, haemorrhage, and vasogenic oedema^[36]. KKS plays a biological role by activating two G protein-coupled receptors known as bradykinin B1 receptor (BDKRB1) and bradykinin B2 receptor (BDKRB2)^[37-38]. Ma *et al*^[39] found that both BDKRB1 and BDKRB2 are present in the human retina, and the level of BDKRB1 is increased in the retina of streptozotocin (STZ)-induced diabetic rats. The proinflammatory effect of KKS on the retina is mainly attributed to BDKRB1^[38,40]. In the STZ-induced diabetic rat model, R715, which is a BDKRB1 antagonist, inhibited retinal vascular permeability and plasma exudation in the experimental group of rats^[41]. Furthermore, R715 administered through eye drops can also reduce leukocyte infiltration and reduce the expression of potential inflammatory mediators in the retina in diabetic rats, including iNOS, COX-2 and IL-1 β . In addition, in endothelial cells and inflammatory cells, BDKRB1 can induce immunogenic responses, increase NF- κ B activity, and produce inflammatory cytokines^[42]. These findings indicate that BDKRB1 is involved in inflammation, and we cannot rule out an association between BDKRB1 and SIG.

PMCH is proteolyzed to produce various peptides, including the appetite hormone melanin-concentrating hormone (MCH)^[43]. It is related to many fundamental physiological processes, such as stress response, metabolic regulation and sleep^[44]. At present, there are few studies on PMCH and ocular diseases, and additional research is necessary.

In any case, these results are valuable because defining these networks provides a framework to confirm that specific genes (*BDKRB1* and *PMCH*) are involved in the process and ultimately interact with the key molecules by which DEX affects the TM.

ACKNOWLEDGEMENTS

Conflicts of Interest: Wei M, None; Chen LM, None; Huang ZY, None; Zhang GW, None; Guan HJ, None; Ji M, None.

REFERENCES

- 1 François J. Corticosteroid glaucoma. *Ophthalmologica* 1984;188(2): 76-81.
- 2 Roberti G, Oddone F, Agnifili L, Katsanos A, Michelessi M, Mastropasqua L, Quaranta L, Riva I, Tanga L, Manni G. Steroid-induced glaucoma: epidemiology, pathophysiology, and clinical management. *Surv Ophthalmol* 2020;65(4):458-472.
- 3 Raghunathan VK, Morgan JT, Park SA, Weber D, Phinney BS, Murphy CJ, Russell P. Stiffens trabecular meshwork, trabecular meshwork cells, and matrix. *Invest Ophthalmol Vis Sci* 2015;56(8):4447-4459.
- 4 Buffault J, Labbé A, Hamard P, Brignole-Baudouin F, Baudouin C. The trabecular meshwork: structure, function and clinical implications. A review of the literature. *J Fr Ophthalmol* 2020;43(7):e217-e230.
- 5 Sbardella D, Tundo GR, Coletta M, Manni G, Oddone F. Dexamethasone downregulates autophagy through accelerated turn-over of the ulk-1 complex in a trabecular meshwork cells strain: insights on steroid-induced glaucoma pathogenesis. *Int J Mol Sci* 2021;22(11):5891.
- 6 Li GR, Lee C, Agrahari V, Wang K, Navarro I, Sherwood JM, Crews K, Farsiou S, Gonzalez P, Lin CW, Mitra AK, Ethier CR, Stamer WD. *In vivo* measurement of trabecular meshwork stiffness in a corticosteroid-induced ocular hypertensive mouse model. *Proc Natl Acad Sci U S A* 2019;116(5):1714-1722.
- 7 Feroze KB, Khazaeni L. *Steroid Induced Glaucoma*. StatPearls. Treasure Island (FL) 2022.
- 8 Dai M, Hu ZL, Kang ZF, Zheng ZK. Based on multiple machine learning to identify the ENO2 as diagnosis biomarkers of glaucoma. *BMC Ophthalmol* 2022;22(1):155.
- 9 Zhao B, Wang MY, Xu J, Li M, Yu YH. Identification of pathogenic genes and upstream regulators in age-related macular degeneration. *BMC Ophthalmol* 2017;17(1):102.
- 10 Matsuda A, Asada Y, Takakuwa K, Sugita J, Murakami A, Ebihara N. DNA methylation analysis of human trabecular meshwork cells during dexamethasone stimulation. *Invest Ophthalmol Vis Sci* 2015;56(6):3801-3809.
- 11 Faralli JA, Desikan H, Peotter J, Kanneganti N, Weinhaus B, Filla MS, Peters DM. Genomic/proteomic analyses of dexamethasone-treated human trabecular meshwork cells reveal a role for GULP1 and ABR in phagocytosis. *Mol Vis* 2019;25:237-254.
- 12 Ritchie ME, Phipson B, Wu D, Hu YF, Law CW, Shi W, Smyth GK. Limma Powers differential expression analyses for RNA-sequencing and microarray studies. *Nucleic Acids Res* 2015;43(7):e47.
- 13 Jiao XL, Sherman BT, Huang DW, Stephens R, Baseler MW, Lane HC, Lempicki RA. DAVID-WS: a stateful web service to facilitate gene/protein list analysis. *Bioinformatics* 2012;28(13):1805-1806.
- 14 Kanehisa M, Furumichi M, Tanabe M, Sato Y, Morishima K. KEGG: new perspectives on genomes, pathways, diseases and drugs. *Nucleic Acids Res* 2017;45(D1):D353-D361.
- 15 Song XD, Du R, Gui H, Zhou M, Zhong W, Mao CM, Ma J. Identification of potential hub genes related to the progression and prognosis of hepatocellular carcinoma through integrated bioinformatics analysis. *Oncol Rep* 2020;43(1):133-146.
- 16 Szklarczyk D, Franceschini A, Wyder S, et al. STRING v10: protein-protein interaction networks, integrated over the tree of life. *Nucleic Acids Res* 2015;43(Database issue):D447-D452.
- 17 Li C, Li JQ, Lu PR. Identification of key genes involved in Brg1 mutation-induced cataract using bioinformatics analyses with publicly available microarray data. *Acta Biochim Pol* 2021;68(4):733-737.
- 18 Mohd Nasir NA, Agarwal R, Krasilnikova A, Sheikh Abdul Kadir SH, Iezhita I. Effect of dexamethasone on the expression of MMPs, adenosine A1 receptors and NFKB by human trabecular meshwork cells. *J Basic Clin Physiol Pharmacol* 2020;31(6).
- 19 Yemany F, Baidouri H, Burns AR, Raghunathan V. Dexamethasone and glucocorticoid-induced matrix temporally modulate key integrins, caveolins, contractility, and stiffness in human trabecular meshwork cells. *Invest Ophthalmol Vis Sci* 2020;61(13):16.
- 20 Wu AN, Khawaja AP, Pasquale LR, Stein JD. A review of systemic medications that may modulate the risk of glaucoma. *Eye (Lond)* 2020;34(1):12-28.
- 21 Griffin S, Boyce T, Edmunds B, Hills W, Grafe M, Tehrani S. Endogenous hypercortisolism inducing reversible ocular hypertension. *Am J Ophthalmol Case Rep* 2019;16:100573.
- 22 Choi KJ, Na YJ, Jung WH, Park SB, Kang S, Nam HJ, Ahn JH, Kim KY. Protective effect of a novel selective 11 β -HSD1 inhibitor on eye ischemia-reperfusion induced glaucoma. *Biochem Pharmacol* 2019;169:113632.
- 23 Patel GC, Millar JC, Clark AF. Glucocorticoid receptor transactivation is required for glucocorticoid-induced ocular hypertension and glaucoma. *Invest Ophthalmol Vis Sci* 2019;60(6):1967-1978.
- 24 Chan WL, Wiggs JL, Sobrin L. The genetic influence on corticosteroid-induced ocular hypertension: a field positioned for discovery. *Am J Ophthalmol* 2019;202:1-5.
- 25 Guichard A, Humbert P, Tissot M, Muret P, Courderot-Masuyer C, Viennet C. Effects of topical corticosteroids on cell proliferation, cell cycle progression and apoptosis: *in vitro* comparison on HaCaT. *Int J Pharm* 2015;479(2):422-429.
- 26 Chang MC, Kuo YJ, Hung KH, Peng CL, Chen KY, Yeh LK. Liposomal dexamethasone-moxifloxacin nanoparticle combinations

- with collagen/gelatin/alginate hydrogel for corneal infection treatment and wound healing. *Biomed Mater* 2020;15(5):055022.
- 27 Bogarin T, Saraswathy S, Akiyama G, Xie XB, Weinreb RN, Zheng J, Huang AS. Cellular and cytoskeletal alterations of scleral fibroblasts in response to glucocorticoid steroids. *Exp Eye Res* 2019; 187:107774.
- 28 Gordon MO, Kass MA. What we have learned from the ocular hypertension treatment study. *Am J Ophthalmol* 2018;189:xxiv-xxvii.
- 29 Vranka JA, Kelley MJ, Acott TS, Keller KE. Extracellular matrix in the trabecular meshwork: intraocular pressure regulation and dysregulation in glaucoma. *Exp Eye Res* 2015;133:112-125.
- 30 Li GR, Cui G, Dismuke WM, Navarro I, Perkumas K, Woodward DF, Stamer WD. Differential response and withdrawal profile of glucocorticoid-treated human trabecular meshwork cells. *Exp Eye Res* 2017;155:38-46.
- 31 Overby DR, Clark AF. Animal models of glucocorticoid-induced glaucoma. *Exp Eye Res* 2015;141:15-22.
- 32 Muralidharan AR, Maddala R, Skiba NP, Rao PV. Growth differentiation factor-15-induced contractile activity and extracellular matrix production in human trabecular meshwork cells. *Invest Ophthalmol Vis Sci* 2016;57(15):6482-6495.
- 33 Kameda T, Zvick J, Vuk M, Sadowska A, Tam WK, Leung VY, Bölskei K, Helyes Z, Applegate LA, Hausmann ON, Klasen J, Krupkova O, Wuertz-Kozak K. Expression and activity of TRPA1 and TRPV₁ in the intervertebral disc: association with inflammation and matrix remodeling. *Int J Mol Sci* 2019;20(7):E1767.
- 34 Paiva ACM, da Fonseca AS. Could adverse effects and complications of selective laser trabeculoplasty be decreased by low-power laser therapy? *Int Ophthalmol* 2019;39(1):243-257.
- 35 Fini ME, Schwartz SG, Gao XY, Jeong S, Patel N, Itakura T, Price MO, Price FW Jr, Varma R, Stamer WD. Steroid-induced ocular hypertension/glaucoma: focus on pharmacogenomics and implications for precision medicine. *Prog Retin Eye Res* 2017;56:58-83.
- 36 Liu WJ, Stanton RC, Zhang ZY. The kallikrein-kinin system in diabetic kidney disease. *Curr Opin Nephrol Hypertens* 2017;26(5):351-357.
- 37 Matus CE, Ehrenfeld P, Pavicic F, González CB, Concha M, Bhoola KD, Burgos RA, Figueroa CD. Activation of the human keratinocyte B1 bradykinin receptor induces expression and secretion of metalloproteases 2 and 9 by transactivation of epidermal growth factor receptor. *Exp Dermatol* 2016;25(9):694-700.
- 38 Martin RP, Filippelli-Silva R. Non-radioactive binding assay for bradykinin and angiotensin receptors. *Methods Cell Biol* 2019;149:77-85.
- 39 Ma JX, Song Q, Hatcher HC, Crouch RK, Chao L, Chao J. Expression and cellular localization of the kallikrein-kinin system in human ocular tissues. *Exp Eye Res* 1996;63(1):19-26.
- 40 Pouliot M, Talbot S, Sénécal J, Dotigny F, Vaucher E, Couture R. Ocular application of the kinin B1 receptor antagonist LF22-0542 inhibits retinal inflammation and oxidative stress in streptozotocin-diabetic rats. *PLoS One* 2012;7(3):e33864.
- 41 Brondani LA, Crispim D, Pisco J, Guimarães JA, Berger M. The G allele of the rs12050217 polymorphism in the *BDKRBI* gene is associated with protection for diabetic retinopathy. *Curr Eye Res* 2019;44(9):994-999.
- 42 Sun DP, Lee YW, Chen JT, Lin YW, Chen RM. The bradykinin-*BDKRBI* axis regulates aquaporin 4 gene expression and consequential migration and invasion of malignant glioblastoma cells via a Ca²⁺-MEK1-ERK1/2-NF-κB mechanism. *Cancers* 2020;12(3):667.
- 43 Angulo-Valenzuela NI, Thomas MG, Riley DG, Medrano JF, Reyna-Granados JR, Aguilar-Trejo CM, Luna-Nevárez P. A SNP within the *PMCH* gene as a molecular marker associated with fertility traits in Angus and Brangus beef heifers raised under a desert environment. *Trop Anim Health Prod* 2021;53(3):355.
- 44 Battagello DS, Lorenzon AR, Diniz GB, et al. The rat mammary gland as a novel site of expression of melanin-concentrating hormone receptor 1 mRNA and its protein immunoreactivity. *Front Endocrinol (Lausanne)* 2020;11:463.